

Assessment of airborne scanning laser altimetry (lidar) in a deltaic wetland environment

Jessika Töyrä, Alain Pietroniro, Christopher Hopkinson, and William Kalbfleisch

Abstract. The objective of the study was to evaluate the airborne scanning light detection and ranging (lidar) technology for hydrological applications in wetlands, deltas, or other similar areas. A comparison of lidar data with in situ survey data revealed a negative elevation bias of 0.21 m, which was corrected by block adjustment. The evaluation demonstrated that the lidar pulses had difficulties penetrating thick willow cover and dense thatch layers beneath the grasses and sedges (graminoids). After block adjustment, the lidar data achieved a root mean squared error (RMSE) of 0.15 and 0.26 m in graminoid and willow vegetation, respectively. The bare ground points produced an RMSE of 0.07 m. To be useful in hydrologic modelling, elevation data need to be interpolated into an even grid, or a digital elevation model (DEM). Four interpolation algorithms were evaluated for accuracy. The input elevations were best honoured when interpolated into a 0.25 m grid using a kriging algorithm and, thereafter, averaged to a 4 m resolution DEM. The RMSE of the DEM was 0.22 m. Despite some problems in dense vegetation, the lidar DEM provided useful topographic detail in a resolution and accuracy that is acceptable for many hydrologic purposes.

Résumé. L'objectif de cette étude était d'évaluer la technologie de balayage lidar aéroporté pour les applications hydrologiques dans les terres humides, les deltas ou autres régions similaires. Une comparaison des données lidar par rapport aux données in situ de relevés de terrain a révélé un biais négatif d'altitude de 0,21 m, qui a été corrigé par ajustement de blocs. L'évaluation a démontré que les pulsations lidar ont eu de la difficulté à pénétrer le couvert épais de saules et les couches denses de chaume sous les herbes et les laïches (graminées). Après l'ajustement de blocs, les données lidar ont atteint une valeur de RMSE respectivement de 0,15 et 0,26 m pour la végétation de graminées et de saules. Les points de sol nu ont donné un RMSE de 0,07 m. Pour être utile en modélisation hydrologique, les données d'altitude doivent être interpolées dans une grille régulière ou un modèle numérique d'altitude (MNA). Quatre algorithmes d'interpolation ont été évalués pour leur précision. Les altitudes d'entrée étaient davantage mises en valeur lorsque interpolées dans une grille de 0,25 m à l'aide d'un algorithme de krigeage, et ensuite moyennées par rapport à un MNA d'une résolution de 4 m. La valeur de RMSE du MNA était de 0,22 m. En dépit de certains problèmes dans le cas de la végétation dense, le MNA lidar fournit des détails topographiques utiles avec une résolution et une précision qui sont acceptables pour plusieurs besoins hydrologiques.

[Traduit par la Rédaction]

Introduction

The Peace–Athabasca Delta is a 3900 km² wetland complex located in northeastern Alberta at the confluence of the Peace and Athabasca rivers. The small wetland basins scattered within the delta provide important habitat for a large number of waterfowl that migrate northward along four major North American flyways. Numerous muskrats also rely on the shallow wetland basins for survival, and a large free-roaming herd of wood bison graze on the grasses and sedges in the delta. Since a major portion of the wetland basins is disconnected from the channel network, they will have to rely on large, periodic overland floods to replenish and maintain their productivity. The hydrology of the Peace–Athabasca Delta has received much attention during the past 30 years (PADPG, 1973; PADIC, 1987; PADTS, 1996), mainly because of the concern that the construction of the W.A.C. Bennett dam and Williston Reservoir on the Peace River in 1968 would affect the flood frequency and, thereby, also the ecosystem of the wetland complex. The ecology of the Peace–Athabasca Delta is driven by the hydrologic regime, and many studies have been undertaken to assess the effect of the flood frequency

on the vegetation patterns (PADPG, 1973; PADTS, 1996). PADPG (1973) proposed that reduced flooding and declining water levels would allow encroaching willows to advance into the wetland basins and replace the productive emergent vegetation. Timoney (2002), on the other hand, suggested that the wetland ecology is much more resistant to change than previously believed.

Our research has focused on mapping, monitoring, and understanding the extent, frequency, and duration of flooding within the Peace–Athabasca Delta for the purposes of ecosystem assessment and management. This involves monitoring past changes and developing predictive hydrological models to

Received 31 January 2003. Accepted 24 July 2003.

J. Töyrä¹ and **A. Pietroniro**. National Water Research Institute, 11 Innovation Boulevard, Saskatoon, SK S7N 3H5, Canada.

C. Hopkinson. Laboratory for Remote Sensing of Earth & Environmental Systems, Queen's University, 99 University Avenue, Kingston, ON K7L 3N6, Canada.

W. Kalbfleisch. Optech Incorporated, 100 Wildcat Road, Toronto, ON M3J 2Z9, Canada.

¹Corresponding author (e-mail: jessika.toyra@ec.gc.ca).

assess potential future change resulting from either a modified operating regime of the Williston Reservoir, or climatic forcing due to climate change. A one-dimensional hydrodynamic model (ONE-D model; see B.C. Environment and Environment Canada, 1995) linked with the WATFLOOD hydrological model (Kouwen, 1988) has been used in the Peace–Athabasca Delta to assess possible strategies for improved water management and to further the understanding of climatic and anthropogenic influences within the area. The large size, unique terrain, and remoteness of the delta along with a lack of detailed and accurate topographic information and poor hydrometric records pose a challenge to understanding the hydrology and applying the models. As such, it also presents an ideal opportunity for employing remote sensing as a hydrologic monitoring tool, an approach that is too often overlooked in many water-management studies (Kite and Pietroniro, 1996).

To understand the movement of water within the connected and nonconnected channels and basins, detailed and accurate digital elevation information is required. For this purpose, airborne scanning light detection and ranging (lidar) data were evaluated for accuracy and utility. The Peace–Athabasca Delta has a very low relief, with the exception of the channel levees and some scattered bedrock outcrops. This presents a modelling problem, since small water level changes can result in a large increase in water surface area. It also becomes difficult to predict at what water level isolated basins will flood or to determine the point of flooding (the spillway). Elevation models derived from 1:50 000 scale contour lines and survey points have been used up to date. These elevation models lack the detail and accuracy needed for flood forecasting. Traditional in situ surveying is impossible for such a large area with such difficult terrain. Airborne stereophotography is possible but is very time consuming and costly. Airborne scanning lidar sensors have the potential to provide accurate data at high densities. As of 1997, point densities of 100 000/km² or one point per 10 m² were standard (Flood and Gutelius, 1997) and could be achieved for large areas. Today, densities better than one point per 1 m² are possible at 1000 m above ground level (agl) with 50 kHz pulse rate systems (Optech Incorporated, personal communication).

The airborne lidar sensor transmits and receives light pulses at a high frequency, and the position and elevation of each pulse can be calculated based on the position of the aircraft and the time it takes for the pulse to return from the ground. The position of the aircraft is determined based on differential global positioning system (GPS) measurements and an inertial navigation system (INS). This technology has been previously tested for applications such as prediction of forest stand characteristics (Means et al., 2000), beach topography mapping (Mason et al., 2000), and ice sheet and glacier topography mapping (Krabill et al., 1995; Hopkinson et al., 2001). The accuracy reported by the manufacturer (Optech Incorporated, 2000) over hard, unambiguous surfaces is 1/2000 × sensor altitude in the horizontal direction, and the vertical accuracy is reported as 0.15 and 0.20 m for sensor altitudes of 1200 and

1500 m agl, respectively. These accuracy values were based on 1 σ measurements, that is, the standard deviation of the differences between lidar and verification elevations. Bowen and Waltermire (2002) pointed out that most lidar evaluations were conducted over nonvegetated terrain with very low local relief. Bowen and Waltermire (2002) evaluated scanning lidar data in variable terrain along river corridors and found that the vertical error was about 0.20 m higher than previously reported for flat terrain, which they attributed to horizontal positioning limitations. This study focuses on evaluating the use of scanning lidar for mapping wetland topography, where the elevation changes are slight, except for levees and outcrops, and the vegetation cover varies from bare mud to very dense willows.

Study sites

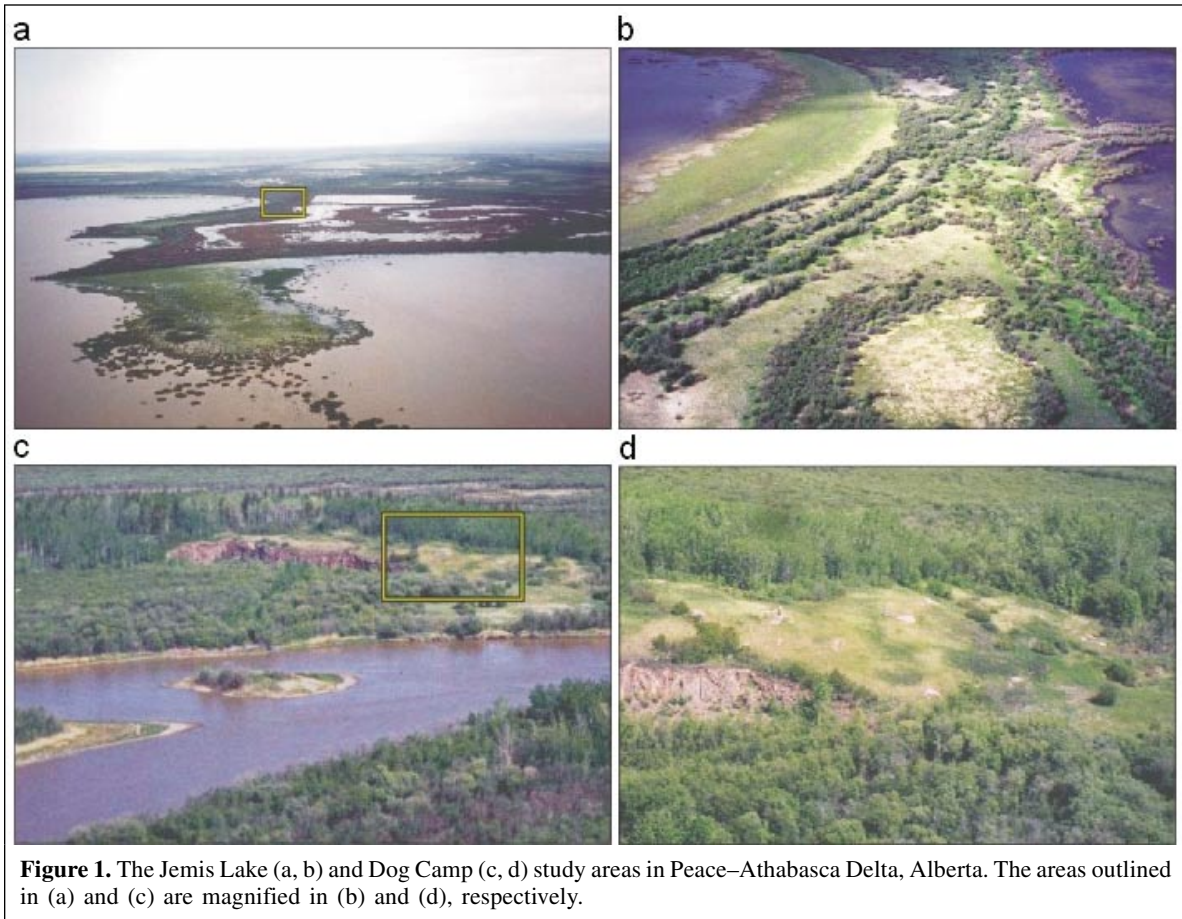
Jemis Lake is a wetland basin that is separated from Mamawi Lake by a relatively low levee. There is no open connection between the two basins, and Jemis Lake has to depend on large overland floods to get replenished. As in the case of most of the Peace–Athabasca Delta, the topography of the Jemis Lake basin is very flat (see **Figure 1a**). When the lidar survey was conducted, the low-lying areas were still filled with water from the 1996 and 1997 floods. As illustrated in **Figure 1b**, the basin is characterized by bands of dense willows (*Salix*) and areas covered by grasses (*Calamagrostis* and *Scolochloa*) and sedges (*Carex*). These are also the dominating vegetation types in the Peace–Athabasca Delta, making the basin ideal as a test area. The lidar acquisition was conducted in the middle of June 2002, and many of the willows were already partially foliated. There was also some bare mud exposed, as the water levels were receding.

As mentioned, most of the delta is relatively flat, with the exception of some higher levees and bedrock outcrops. To evaluate the scanning lidar on steeper topography, the other test site was established on the slope of a large bedrock outcrop in the Dog Camp area. Dog Camp is covered by grasses, sedges, and willows (see **Figures 1c, 1d**).

Methodology

Vertical reference

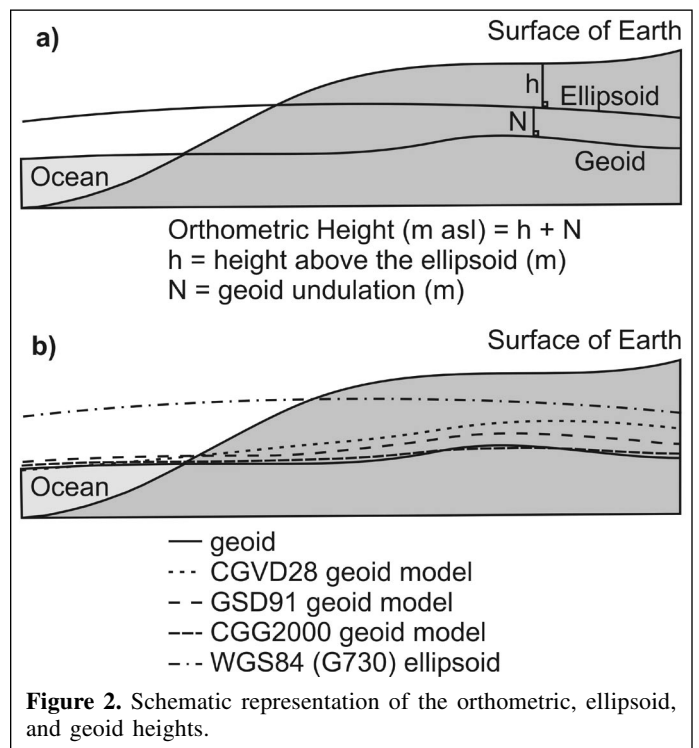
When conducting a high-precision survey or comparing elevation data from different sources it is important to know what vertical datum or geoid model the data were referenced to. **Figure 2a** illustrates the relationship between the earth's surface, an ellipsoid, and the geoid. The geoid is an equipotential surface close to the mean sea level, and the direction of gravity is perpendicular to its surface. The ellipsoid is an elliptical surface that is used to approximate the geoid. Orthometric heights represent the elevation above the geoid, or above sea level. Based on the relationship in **Figure 2a**, the orthometric height (H) can be calculated using the following



equation if the ellipsoid height (h) and geoid height (N) are known:

$$H = h - N \quad (1)$$

In Canada, the official vertical datum is the Canadian Geodetic Vertical Datum of 1928 (CGVD28), which means that the orthometric heights of all the first-order vertical benchmarks are based on this datum. The CGVD28 datum was determined in 1928 using very precise levelling techniques and the mean sea level at six locations along the Atlantic and Pacific coasts as constraints. Since then, all spirit levelling observations are constrained to this datum, forming now a network of some 80 000 benchmarks (Véronneau et al., 2001). Because of isostatic rebound following the last glaciation, rise in mean sea level, and other systematic errors, the CGVD28 orthometric heights do not represent the true heights above the geoid (see **Figure 2b**). More recent national geoid models, GSD91, GSD95, and CGG2000, were developed by the Geodetic Survey Division (GSD), Natural Resources Canada, based on gravimetric measurements. These models describe the geoid height at any point in Canada. Each version of the geoid model represents the geoid height more accurately because of



enhanced theory and data collection. The resolution of the CGG2000 model is 2 min of an arc in both latitude and longitude, and the calculated mean absolute error for all of Canada is 0.18 m (1σ) (Véronneau et al., 2001; Véronneau, 2002). Additional information about these models can be found in Véronneau (1997; 2002), Véronneau et al. (2001), and Vergos and Sideris (2002).

If a GPS-derived ellipsoid height (WGS84 G730) is obtained and the geoid undulation is determined using the latest geoid model (CGG2000), the calculated orthometric height will not equal the CGVD28 orthometric height. Because of this, the Geodetic Survey Division developed height transformations for the GSD95 and CGG2000 geoid models that adjust for the differences and allow CGVD28 orthometric heights to be determined from GPS-derived ellipsoid heights (Véronneau et al., 2001).

Since the objective of this project was to evaluate the use of lidar data to predict the flow of water in the wetland area, it was more important to retrieve elevation data based on heights above the geoid rather than an official orthometric datum. Therefore, it was decided that the datasets in this study should be referenced to the CGG2000 geoid model.

Lidar data survey

The lidar survey was conducted over the study sites on 17 June 2000 using an ALTM 1225 airborne scanner operating at a wavelength of 1064 nm. The position of the aircraft and scanning lidar was calculated based on data from an onboard geodetic-grade GPS receiver and an INS. Another geodetic-grade GPS receiver, located on a known benchmark, was used for differential correction of the aircraft GPS. The ground station GPS was located less than 20 km away from the aircraft at any point during the lidar survey. Ground positional coordinates and ellipsoid heights were computed for each lidar pulse based on the position of the aircraft and the time it took for the transmitted lidar pulse to return from the ground. For each transmitted pulse, the sensor recorded the return time of the first returning pulse and the last returning pulse. This means that two elevations were obtained for every transmitted pulse. In heavily vegetated areas, the first pulse often represents the top of vegetation and the last pulse may represent either vegetation or ground depending on if it was able to penetrate the entire canopy. In more open areas, the first and last pulse may both represent ground elevations. The coordinates were referenced to the Universal Transverse Mercator (UTM, zone 12) projection based on the WGS84 datum. The lidar elevations were provided as WGS84 (G730) ellipsoid heights. The lidar survey was conducted at a flying altitude of 1300 m agl, for which the vertical and horizontal accuracies on bare, level surfaces are quoted as 0.17 and 0.65 m, respectively. The ALTM settings are listed in **Table 1**.

TerraScan software was used to remove the points that did not completely penetrate the vegetation, leaving only the points representing the ground surface. To obtain a denser dataset, both first and last pulse data were combined and used as input

Table 1. ALTM 1225 airborne scanner settings for the lidar survey.

Parameter	Setting
Altitude (m above ground level)	1300
Air speed (kn)	95–115
Laser pulse rate (kHz)	25
Scan frequency (Hz)	18
Max. scan angle (°)	20

in the vegetation-removal process. The evaluation was conducted on the points that represented ground elevations.

Datasets containing *X–Y–Z* data points were created for the two study areas. The horizontal distance between adjacent lidar ground points ranged between 0.25 m and several metres. The higher point densities generally occurred where two scan swaths overlapped. In cases where the first and last pulses reached the ground and were both included in the ground dataset, two points could be as close as a few centimetres from each other. These points were very close in elevation, however, and were thus regarded as the same point. Because of the high point density, the Jemis Lake study area was divided into six 3 km × 3 km patch files. Some of these patch files still contain over one million points. The Dog Camp study area is small and was covered by one 3 km × 3 km patch file.

Ground verification data survey

The lidar survey was conducted in the early summer when the changes in vegetation density and height are relatively rapid. To enable accuracy assessment of lidar data, in situ elevation surveys were conducted at the two study sites. These ground measurements were carried out only a day prior to the lidar survey to ensure that accurate environmental conditions were recorded. The ground surveys were conducted using a total station instrument. A permanent rod was used as the survey instrument site for the Jemis Lake area. The position of this site was determined in 1995 (Lavergne, 1995) and again in 2000 using differential GPS. A temporary rod was established as a backsite for the total station, and its position was determined using differential GPS. Benchmarks with known coordinates were used as instrument site and backsite for the Dog Camp area. The horizontal survey coordinates were referenced to the UTM zone 12 projection based on the WGS84 datum. The orthometric heights were based on the GSD91 geoid model. Conservative estimates of the vertical and horizontal accuracy of the survey data are 0.10 and 0.15 m, respectively.

Since the lidar pulses do not penetrate water, the survey was conducted in dry areas. To assess the vegetation-penetration capabilities of the scanning lidar, transects and scattered points were surveyed in different vegetation types, ranging from bare mud to dense grasses and willows. The height and leaf area index (LAI) of the vegetation cover were measured at representative sites.

Additional total station survey points in Jemis Lake basin from 1996 (Carter, 1996) were also used for the lidar evaluation.

The vegetation cover on these points was determined using a 4 m resolution multispectral IKONOS image acquired 12 days prior to the lidar survey. The IKONOS image was also used to exclude any points located in flooded areas. The IKONOS image covers all of the Dog Camp area and most of the Jemis Lake area and was used as another tool for the evaluation. All survey points included, there were a total of 12 bare mud survey points, 71 points in graminoid (grasses and sedges) vegetation cover, 53 survey points in willow bushes, and nine points in dead willows.

Lidar data evaluation

Prior to evaluation, both datasets were converted into CGG2000 orthometric heights. The lidar elevations were provided as WGS84 (G730) ellipsoid heights and could be converted directly into orthometric heights using the geoid information from the CGG2000 model. The survey data were obtained as GSD91 orthometric heights, which meant that they first had to be converted into WGS84 ellipsoid heights using geoid data from the GSD91 geoid model and then converted back into orthometric heights based on the CGG2000 geoid model. When both datasets were referenced to a common model, the lidar points could be compared with the ground survey points. For both study sites, the lidar points located closest to each of the survey points were selected and used for the evaluation. The survey elevations were subtracted from the lidar elevations to retrieve the following statistical error measurements: root mean squared error (RMSE), average difference (AvD), and maximum absolute difference (MaxAD). The average difference indicates if there is any systematic elevation bias in the lidar data. If a bias was found for points on bare ground, the lidar elevations were block adjusted to compensate for the bias prior to data gridding.

Lidar data gridding

To create a digital elevation model (DEM), the lidar point data needed to be interpolated into an even grid where each grid cell would contain an elevation value. As mentioned previously, the smallest spacing between the lidar points was

approximately 0.25 m. To retain the detailed topographical information, the grid cell size should be set to the smallest spacing of the input elevation points. A grid cell size of 0.25 m, however, would produce very large files that are difficult to manage. One 3 km × 3 km patch file would create a grid with 12 000 × 12 000 cells. It would, for example, be unreasonable to create a 0.25 m resolution DEM of Jemis Lake, since it requires 24 000 × 36 000 grid cells. A cell size of 4 m was preferred, since it would reduce the Jemis Lake DEM to 1500 × 2250 grid cells, which is a more manageable size. A 4 m DEM would also match the IKONOS image resolution.

Since the grid cell size was set to 4 m and the input data spacing was anywhere between 0.25 m and several metres, the interpolation process became difficult. Preferably, the values should be averaged when there are many data points within a grid cell and interpolated from adjacent points when there are no data points within a grid cell. A combination of interpolation and averaging was achieved by gridding the individual patch files into 0.25 m DEMs and aggregating (average) them up into 4 m DEMs. The 4 m DEMs were then merged together into a larger mosaic. Three interpolation algorithms were tested for accuracy: kriging, inverse distance to power, and triangulation (TIN). Because of software constraints, only the kriging algorithm could be used to grid the patch files into 0.25 m grid cells, which were then averaged up to 4 m grid cells. For comparison, all three algorithms were used to grid the data directly into 4 m grid cells. In total, four 4 m resolution DEMs were created. One of the Jemis Lake patch files was used for the evaluation of the different gridding methods. **Figure 3** illustrates the gridding process.

The kriging technique (Cressie, 1993) interpolates values by calculating the weighted sum of known points. The weights are determined by considering the covariance between any two known points and between the unknown point and each of the known points. A spherical variogram with a nugget of 0 and a sill of 1 was used by the algorithm to determine the covariances. The range was set automatically to the average distance between known points. An RTREE blocking method was used with a maximum number of seven points in each

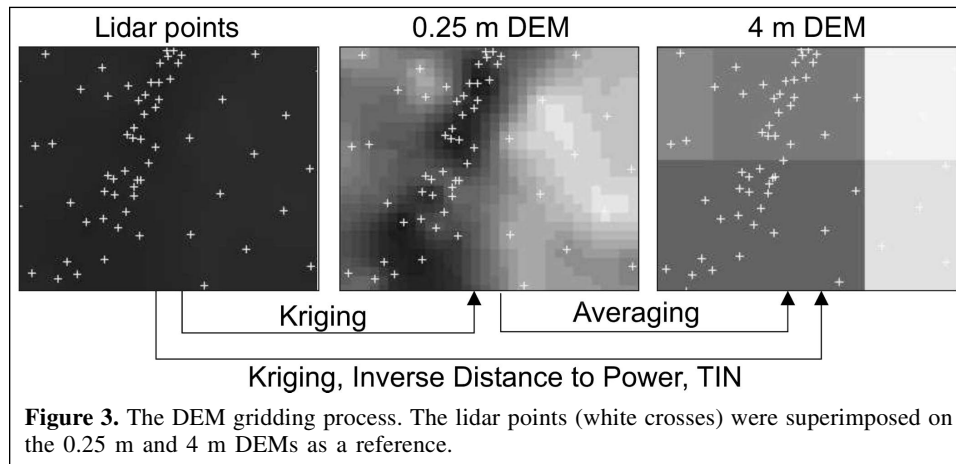


Figure 3. The DEM gridding process. The lidar points (white crosses) were superimposed on the 0.25 m and 4 m DEMs as a reference.

block. The RTREE algorithm splits the block along its major axis when the maximum number of points is exceeded.

The inverse distance to power grid was created using a search radius of 2 m. A value was only to be calculated if there was one or more input elevation points within the radius. This means that the points closest to the centre of a 4 m grid cell had more influence on the output value than those by the edge. The grid cell was assigned a value of zero if there were no points within the cell. The grid cells with no elevation value were filled in using a morphology-dependent interpolation procedure (MDIP) with a conic search algorithm.

The four DEMs were assessed both visually and quantitatively. To evaluate which interpolation algorithm could best honour the original input elevations, the gridded elevation was extracted at each lidar point from all four DEMs. The difference between actual lidar elevation and gridded elevation was calculated for each lidar point. The interpolation method that produced the lowest RMSE and the most visually pleasing DEM was then used to generate the DEMs for the six patch files over Jemis Lake and the one patch file covering Dog Camp. The six patch files over Jemis Lake were, thereafter, joined into a larger mosaic. The generated DEMs were also compared with survey data by extracting the gridded elevation for each survey point.

Results and discussion

Lidar points

The precise location of the lidar pulse cannot be determined a priori, resulting in the in situ measurements and the lidar estimates rarely coinciding, making direct comparison difficult. Because of this, the horizontal distance between the in situ survey points and the closest lidar point was calculated for each survey–lidar pair that was used for the evaluation. The horizontal distance between two compared points is referred to as $\overrightarrow{XY}_{\text{Diff}}$ in the remainder of the paper. The largest calculated $\overrightarrow{XY}_{\text{Diff}}$ values were 4.4 and 2.6 m for Jemis Lake and Dog Camp, respectively. In Jemis Lake, where the elevation changes were small, a horizontal distance of one to a few metres would not represent a great change in elevation, with the possible exception of the levee around the basin. At the Dog Camp site, however, where the slopes were steeper, a 2 m horizontal distance on the ground could represent an elevation change of several decimetres. A 1 m threshold was set, and only survey–lidar pairs with an $\overrightarrow{XY}_{\text{Diff}}$ value of less than that were used for the evaluation. Within this threshold no correlation between $\overrightarrow{XY}_{\text{Diff}}$ and accuracy could be found.

The LAI and height of the surveyed vegetation types are listed in **Table 2**. **Figure 4** illustrates the elevation differences between lidar and survey data for each land-cover class. A bias in elevation values can occur when there is no control field in which to initially set the sensor ranges prior to the lidar survey. Bare ground is generally used as an indicator of lidar elevation bias. As **Figure 4** indicates, the bare ground lidar elevations were on average lower than the surveyed elevations. Eleven

Table 2. Description of surveyed vegetation types.

Vegetation type	Average	
	LAI	Height (m)
Graminoid (grasses and sedges)	1.30	0.3–0.4
Thatch layer beneath grass and sedge	4.50	0.10–0.15
Willow (above understory)	2.20	4–7
Dead willow (above understory)	0.98	2–5

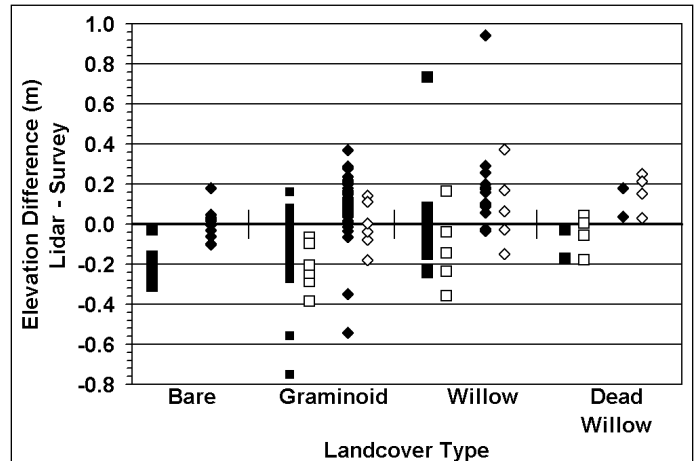


Figure 4. The distribution of differences between lidar and survey elevations for each land-cover class. Only points with an $\overrightarrow{XY}_{\text{Diff}}$ value of less than 1 m were compared. A positive value indicates that the lidar elevation is higher than the surveyed elevation. The squares represent the differences prior to adjustments, and the diamonds represent a comparison between adjusted lidar elevations (+0.21 m) and survey data. The closed and open symbols indicate Jemis Lake and Dog Camp, respectively.

bare ground points were compared in Jemis Lake, and the lidar elevations were on average 0.21 m lower than the surveyed elevations. Therefore, all lidar elevations were raised by 0.21 m to adjust for the negative bias. This is not uncommon, as noted by Bowen and Waltermire (2002). They observed a systematic bias of 0.44 m between their lidar and GPS survey elevations, which they attributed to set-up and calibration errors in the lidar or ground station network.

Figure 4 also illustrates the elevation differences between adjusted lidar and survey data, and **Table 3** shows the error statistics for each land-cover class. **Figure 4** and **Table 3** suggest that the elevation overestimation by the scanning lidar increased as the vegetation height and LAI increased (see **Table 2** for representative LAI measurements). The lidar elevations were on average 0.07 m too high for the points in graminoid vegetation. The graminoid cover was slightly higher and the underlying thatch layer was thicker and denser in Jemis Lake compared with Dog Camp. As **Figure 4** illustrates, the range of differences between lidar and survey elevations was higher for Jemis Lake. The higher range was probably due to the thicker graminoid cover and also because almost eight times more points were surveyed and compared in that study area. The two lidar points in Jemis Lake that were between 0.3 and

Table 3. The error statistics from comparison of the adjusted lidar elevations and the survey elevations for each land-cover class in both study areas.

Statistic	Land-cover class			
	Bare	Graminoid	Willow	Dead willow
AvD	0.00	0.07	0.15	0.14
MaxAD	0.18	0.54	0.94	0.25
RMSE	0.07	0.15	0.26	0.17
N	11	64	22	6

Note: Only points with an XY_{Diff} value of less than 1 m were compared. A positive AvD indicates that the lidar values are on average higher than the surveyed values. AvD, average difference (lidar minus survey); MaxAD, maximum absolute difference; N, sample size; RMSE, root mean squared error.

0.5 m too low were located at the edge of a swath. This issue is addressed in the gridded lidar data section. Only eight lidar points were over 0.20 m too high, and they represented pulses that could not penetrate the entire graminoid cover. The 0.07 m positive bias in the lidar elevations was most likely caused by the thick thatch layer in Jemis Lake. It was, therefore, speculated that the lidar pulses could penetrate the grasses and sedges relatively well but had trouble penetrating dense thatch layers.

The willows were higher and denser than the graminoids, resulting in higher occurrences of lidar pulses reflecting off foliage, branches, stems, or vegetation understory. This was manifested in the average difference statistic, indicating that the adjusted lidar values for willow-covered areas were on average 0.15 m too high. The results also illustrated that the willows had a high range of differences (Figure 4) and the highest MaxAD value (Table 3). Only a few points were surveyed in areas covered by dead willows. The adjusted lidar values were on average 0.14 m higher than the surveyed values for these points. The average difference was similar to that of the willow class, but the spread of differences was less. The lack of foliage in the dead willows should allow the lidar pulse to penetrate the vegetation layer more efficiently.

In addition, the lidar point density was lower in the dense willows. Many of the survey points that were located in willow-covered areas were excluded from the comparison, since there were no lidar points within 1 m radius (the set threshold). As a result of this, only 21% of all the evaluated lidar–survey pairs were located in willow-covered areas in comparison with the 62% that were located in graminoid vegetation. This is the reason why an overall accuracy value was not calculated.

The RMSE value also indicated lower accuracies with increased vegetation thickness. The RMSE in the graminoid vegetation was 0.15 m. When only points in willow vegetation were evaluated, the RMSE increased to 0.26 m. This is again an indication of the difficulty in penetrating dense vegetation. Since the lidar survey was conducted in the early summer after the onset of foliation, the conditions were not ideal for vegetation penetration. A higher accuracy for the willow class may have been attained if the survey was conducted during a leaf-off period. For example, the lidar points in areas covered

by dead willows achieved an RMSE of 0.17 m, which was an improvement from the points in the willow class. The 11 bare ground points produced an RMSE of only 0.07 m.

Gridded lidar data

The four gridding techniques were applied to one of the patch files in Jemis Lake, and the generated 4 m DEMs were evaluated based on how well they could honour the original input values. Table 4 summarizes the error statistics calculated for each DEM when compared with the input lidar elevations. All interpolation methods produced DEMs with RMSEs between 0.07 and 0.09 m, except for the TIN method, which resulted in an RMSE of 0.32 m. The input lidar values were best honoured by gridding the data into 0.25 m grid cells and, thereafter, averaging them up to 4 m cells. With the exception of the TIN DEM, which was very noisy and contained some anomalies (see MaxAD in Table 4), the DEMs had a relatively similar visual appearance and displayed the same trends. A slightly smoother and less noisy DEM was achieved by initially kriging the data into 0.25 m grid cells and then averaging the data. Therefore, this method was selected for lidar data gridding.

The generated 4 m resolution DEMs for Jemis Lake and Dog Camp are illustrated in Figure 5, which also shows the location of the survey points and, as a reference, the IKONOS image for each area. The DEMs provided many details about the two areas, and the levees and channels were detectable in most instances. On the other hand, lidar scan lines and some borders between adjacent swaths are also noticeable in the gridded data (see Figure 6). These elevation artefacts were most likely due to aircraft motion that was not fully compensated for by the INS. More recent systems have higher INS sampling rates, and as this technology improves we expect that such artefacts will largely disappear. The elevation difference between two scan lines was as much as 0.15 m at some locations, and the difference between two adjacent swaths was 0.30 m in the most severe area (see Figure 6b). The 4 m DEM values were also compared with survey data, and the results are listed in Table 5. All available survey data were used for this evaluation. This allowed for a direct point-to-point comparison. The RMSE was higher when the adjusted lidar data were gridded compared with when they were in point form.

Table 4. The average difference (AvD), maximum absolute difference (MaxAD), and root mean squared error (RMSE) between the lidar point elevations and the gridded lidar elevations.

Statistic	Kriging ^a	Kriging ^b	Inverse distance to power and MDIP ^b	Triangulation (TIN) ^b
AvD	0.00	0.00	0.00	0.00
MaxAD	0.92	1.02	1.01	14.40
RMSE	0.07	0.09	0.08	0.32

Note: A total of 1 123 867 points were compared. MDIP, morphology-dependent interpolation procedure.

^aGridded into 0.25 m grid cells and averaged up to 4 m grid cells.

^bGridded into 4 m grid cells.

Transect cross sections

Six survey transects from Jemis Lake and two from Dog Camp were compared with both lidar point data and gridded lidar data. The transect cross sections are illustrated in **Figure 7**. The lidar elevations followed the survey elevations relatively well in most of the Jemis Lake transects (transects 1, 4, and 6). As expected, the lidar point elevations were more variable compared with the gridded elevations, which were levelled out by the interpolation and averaging process. The gridded data lacked many of the unwanted spikes and dips seen in the point data.

Transect 2 illustrates a problem with the vegetation-penetration capabilities combined with an unsuccessful removal of all vegetation points, that is, points representing lidar pulses that were reflected by vegetation instead of the ground. The transect

crossed a levee, and the beginning of the transect (0–40 m) was located in a relatively thick willow cover, whereas the rest of the transect extended through an area of graminoid vegetation. The lidar pulses could not penetrate all the way through the willow cover, and the resulting lidar data points should have been classified as vegetation points and removed from the dataset. The elevation at the beginning of the transect was, therefore, overestimated by almost a metre. A similar problem was encountered along transect 5, which extended along a very slight gentle slope. The transect started in graminoids and ended in dense willow cover. The lidar elevations displayed a sudden increase in elevation at the willow border, which was located at a distance of 30 m. These lidar points should also have been classified as vegetation and removed from the dataset.

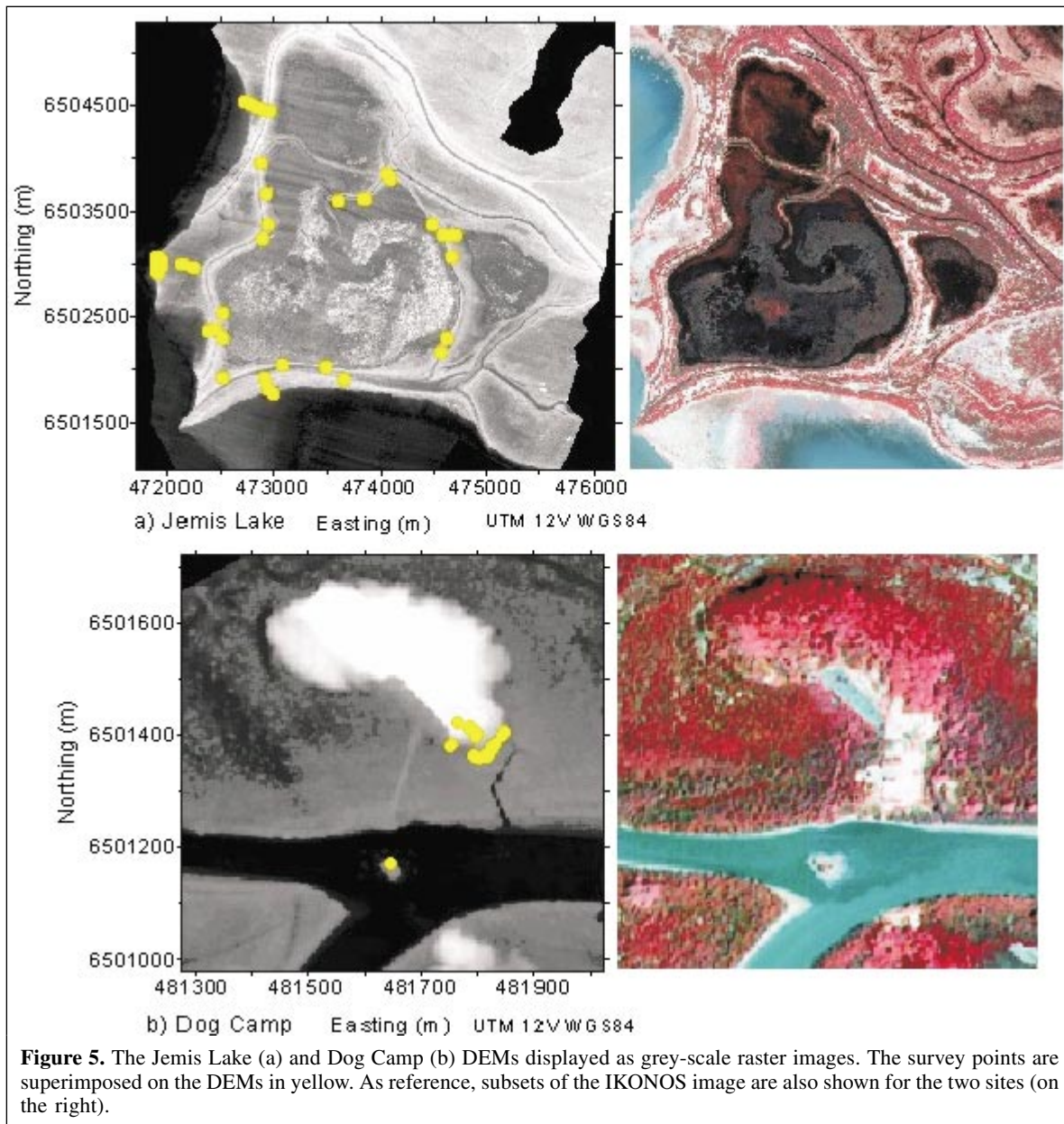


Figure 5. The Jemis Lake (a) and Dog Camp (b) DEMs displayed as grey-scale raster images. The survey points are superimposed on the DEMs in yellow. As reference, subsets of the IKONOS image are also shown for the two sites (on the right).

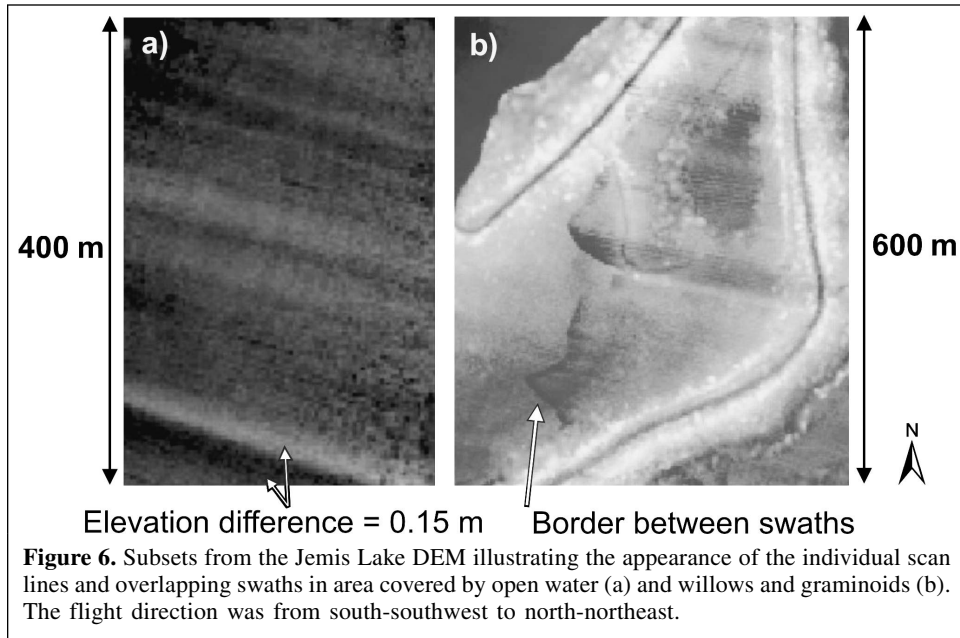


Figure 6. Subsets from the Jemis Lake DEM illustrating the appearance of the individual scan lines and overlapping swaths in area covered by open water (a) and willows and graminoids (b). The flight direction was from south-southwest to north-northeast.

Table 5. The average difference (AvD), maximum absolute difference (MaxAD), and root mean squared error (RMSE) between the gridded lidar elevations (adjusted) and the ground survey elevations.

Statistic	Jemis Lake and Dog Camp	Jemis Lake	Dog Camp
AvD	0.08	0.09	0.00
MaxAD	1.24	1.24	0.69
RMSE	0.22	0.22	0.20
<i>N</i>	145	118	27

Note: All available points were compared. The number of points compared (*N*) is also listed. A positive average difference indicates that the lidar elevations were on average higher than those surveyed.

Transect 3 also extended across a levee, but in this case the beginning and end of the levee were located in graminoid vegetation and the top of the crest (at about 50 m) was covered by thick willows. Transect 3 is an example of where the lidar points could not penetrate the vegetation cover at the top of the crest, and the vegetation-removal algorithm worked correctly and removed the vegetation points. The elevation of the crest was underestimated by more than a metre, however, since the closest lidar ground points were located well below the crest, 4.4 m away from the survey point.

Transects 7 and 8 were located in the Dog Camp site. The lidar points at 60 m distance in transect 7 and at 4.5 m distance in transect 8 were located in thicker willow cover and were not representing true ground points. The elevation spikes caused by these points were removed by the gridding process.

Conclusions

A detailed and accurate elevation model is needed to understand the movement of surface water in the Peace–Athabasca Delta. Scanning lidar data were evaluated for this purpose at two study sites, Jemis Lake and Dog Camp, which were representative of the surrounding wetland complex. The lidar elevation data were evaluated by a comparison with in situ survey data. Both datasets were converted to a common projection and a common vertical reference frame. It is important that the elevation values are orthometric heights based on the same ellipsoid and geoid model. In Canada, the official vertical datum (CGVD28) is not based on gravimetric measurements and does not agree well with the geoid. Since the flow of water is influenced by gravity, it is important to use a more recent and accurate geoid model when calculating orthometric heights for hydrological purposes. This way, a more accurate representation of orthometric heights, and thereby also slopes and river gradients, can be achieved. The WGS84 (G730) ellipsoid and the CGG2000 geoid model were used to calculate the orthometric heights for both datasets.

A comparison with survey points on bare ground indicated that there was a 0.21 m negative bias in the lidar elevations. The bias was compensated for by block adjustment. When dividing the data into land-cover classes, it was noted that the adjusted lidar elevations were on average higher than surveyed elevations for the classes with taller and denser vegetation cover (dense thatch layer, willows, and dead willows). An average elevation bias was calculated for the main vegetation classes. These values could potentially be used to adjust the lidar elevations based on a vegetation map obtained through classification of satellite imagery or other means.

Given the uncertainty and potential sources of error in lidar surveys, it is strongly recommended that verification data be collected in conjunction with lidar surveys. It is also very

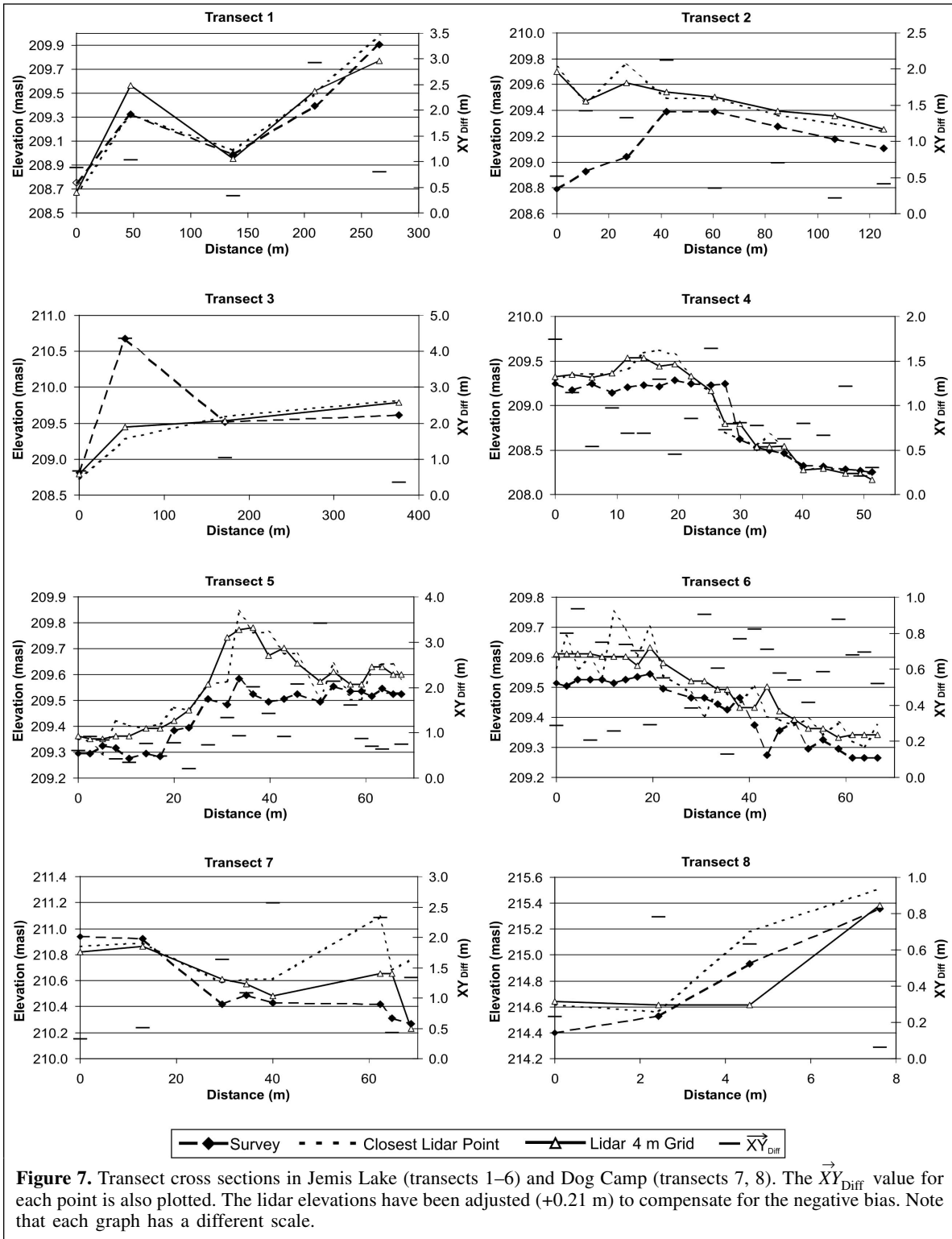


Figure 7. Transect cross sections in Jemis Lake (transects 1–6) and Dog Camp (transects 7, 8). The XY_{Diff} value for each point is also plotted. The lidar elevations have been adjusted (+0.21 m) to compensate for the negative bias. Note that each graph has a different scale.

important that these data are spatially distributed across the study area and in different land-cover types. The results from this study indicated that the RMSE for the adjusted lidar point elevations was 0.15 m in graminoid vegetation and 0.26 m in willow-covered areas. Since the lidar survey was conducted

after the onset of foliation, however, the leaves on the willows resulted in a denser cover and probably reduced the opportunity for complete penetration of the vegetation. Because of this, we also recommend that the scanning lidar surveys in vegetated areas be conducted during leaf-off periods to provide optimal

conditions. More recent scanning lidar systems have higher point densities, which also could increase the opportunity for pulses to penetrate vegetation.

To generate a DEM, the lidar data needed to be interpolated into an even grid. The best results were obtained when the point data were first interpolated into a grid cell size that equalled the smallest horizontal spacing between input points and were thereafter averaged up to the desired resolution. In our case, the kriging method was used to interpolate the points into 0.25 m grid cells, which were averaged into 4 m grid cells. The RMSE of the 4 m grids was found to be 0.22 m. Our research also shows that automated vegetation-removal algorithms in combination with the inability to penetrate thick vegetation resulted in levee heights being occasionally either overestimated through lack of vegetation removal, or underestimated through the lack of ground points on the levee crest. As the levee height is crucial for determining the point and extent of flooding, this could have a negative effect on the modelling of surface water extent at specific water levels. Future applications of lidar in this regime, however, should examine the feasibility of using lidar data in conjunction with LAI or vegetation information to minimize these errors.

Acknowledgements

The authors acknowledge the Northern River Ecosystem Initiative (NREI) and BC Hydro for funding, Wood Buffalo National Park for field logistics, and Kelly Best (National Water Research Institute), Tom Carter (National Water Research Institute), Jay Joyner (BC Hydro), and Graham Lang (BC Hydro) for field support. Tom Carter (National Water Research Institute) provided additional survey points in Jemis Lake, and Optech Incorporated conducted the lidar data acquisition and point data processing. Marc Véronneau, Patrick Legree, and J.C. Lavergne at the Geodetic Survey Division (GSD), Natural Resources Canada, provided invaluable and much appreciated help with geoid models and height transformations. The authors also thank Stephen Gibbard (Prairie Farm Rehabilitation Administration) for processing GPS data and Sheri Korpess and Sheela Selvarasan for data editing and gridding.

References

- Bowen, Z.H., and Waltermire, R.G. 2002. Evaluation of light detection and ranging (lidar) for measuring river corridor topography. *Journal of the American Water Resources Association*, Vol. 38, No. 1, pp. 33–41.
- B.C. Environment and Environment Canada. 1995. *ONE-D hydrodynamic program. Vol. 1 User's manual*. Environment Canada, Ottawa, Ont.
- Carter, T. 1996. Peace–Athabasca Delta perched basin survey. In *Modelling the water balance of Peace–Athabasca Delta perched basins*. Edited by T.D. Prowse, D.L. Peters, and P. Marsh. Peace–Athabasca Delta Technical Studies, Fort Chipewyan, Alta. Appendix 1.
- Cressie, N.A.C. 1993. *Statistics for spatial data*. John Wiley & Sons, Inc., New York.
- Flood, M., and Gutelius, B. 1997. Commercial implications of topographic terrain mapping using scanner airborne laser radar. *Photogrammetric Engineering & Remote Sensing*, Vol. 63, No. 4, pp. 327–364.
- Hopkinson, C., Demuth, M., Sitar, M., and Chasmer, L. 2001. Applications of lidar mapping in a glacierised mountainous terrain. In *Proceedings of the International Geoscience and Remote Sensing Symposium, IGARSS 2001*, 9–14 July 2001, Sydney, Australia. University of New South Wales, Sydney, Australia.
- Kite, G.W., and Pietroniro, A. 1996. Remote sensing applications in hydrological modelling. *Hydrological Sciences*, Vol. 41, No. 4, pp. 563–591.
- Kouwen, N. 1988. WATFLOOD: a micro-computer based flood forecasting system based on real-time weather radar. *Canadian Water Resources Journal*, Vol. 13, No. 1, pp. 62–77.
- Krabill, W.B., Thomas, R.H., Martin, R.N., Swift, R.N., and Frederick, E.B. 1995. Accuracy of airborne laser altimetry over the Greenland ice sheet. *International Journal of Remote Sensing*, Vol. 16, pp. 1211–1222.
- Lavergne, J.C. 1995. *GPS processing and analysis report: Peace–Athabasca Delta Project*. Geodetic Survey Division, Natural Resources Canada, Ottawa, Ont. Project RF3160.
- Mason, D.C., Gurney, C., and Kennett, M. 2000. Beach topography mapping — a comparison of techniques. *Journal of Coastal Conservation*, Vol. 6, pp. 113–124.
- Means, J.E., Acker, S.A., Fitt, B.J., Renslow, M., Emerson, L., and Hendrix, C.J. 2000. Predicting forest stand characteristics with airborne scanning lidar. *Photogrammetric Engineering & Remote Sensing*, Vol. 66, No. 11, pp. 1367–1371.
- Optech Incorporated. 2000. *ALTM 1225 specifications*. Optech Incorporated, Toronto, Ont.
- PADIC. 1987. *Peace–Athabasca Delta: water management works evaluation — final report*. Peace–Athabasca Delta Implementation Committee (PADIC), Governments of Canada, Alberta and Saskatchewan.
- PADPG. 1973. *Peace–Athabasca Delta Project — technical report*. Peace–Athabasca Delta Project Group (PADPG), Edmonton, Alta.
- PADTS. 1996. *Final report November 1996*. Peace–Athabasca Technical Studies (PADTS), Fort Chipewyan, Alta.
- Timoney, K. 2002. A dying delta? A case study of a wetland paradigm. *Wetlands*, Vol. 22, No. 2, pp. 282–300.
- Vergos, G.S., and Sideris, M.G. 2002. Evaluation of geoid models and validation of geoid and GPS/leveling undulations in Canada. *IGeS Bulletin*, Vol. 12, pp. 3–17.
- Véronneau, M. 1997. The GSD95 geoid model for Canada. In *Gravity, Geoid and Marine Geodesy, Proceedings of the International Symposium*, 30 September – 4 October 1996, Tokyo, Japan. Edited by J. Segawa, H. Fujimoto, and S. Okubo. Springer-Verlag, Berlin. Vol. 117, pp. 573–580.
- Véronneau, M. 2002. *The Canadian gravimetric geoid model of 2000 (CGG2000)*. Geodetic Survey Division, Natural Resources Canada, Ottawa, Ont.
- Véronneau, M., Mainville, A., and Craymer, M.R. 2001. *The GPS height transformation (v2.0): An ellipsoidal-CGVD28 height transformation for use with GPS in Canada*. Geodetic Survey Division, Natural Resources Canada, Ottawa, Ont.